D－1　渤海・東シナ海における河川経由の環境負荷が海洋生態系に与える影響評価手法に関する研究

（3）生態系モデルによる環境負荷の影響評価手法に関する総合的研究

③　渤海・東シナ海における河川経由の環境負荷予測に関する国際交流研究

研究代表者　国立環境研究所　水土壌圏環境部　部長　　渡辺正孝

エコフロンティアフェロー　　Wang Quan

平成９年度～１０年度合計予算額　3,525 千円

（平成１０年度予算額　1,765 千円）

[要旨]

中国においては経済発展が急速に進展しており水資源開発、エネルギー開発等の増大、土地利用形態の変化、工業化さらには沿岸域への人工の集中に伴い汚濁物質や有害物質の排出負荷量が著しく増大している。特に河川経由の環境負荷の推定手法の確立は海洋生態系機能および生物種多様性に与える影響を評価する上で重要である。

本研究では NOAA の AVHRR 画像データを用いて 1997 年 10 月に行った長江河口域でのメゾコズム実験期間での海域環境把握と長江河口域での環境負荷の推定を濁度について行った。1997 年 10 月 6 日から 10 月 20 日までの 15 画像を用いて雲の影響を除去しコンポジェット画像を求めた。split-window channel アルゴリズムを用いて海水温 (multi-channel sea surface temperature, MUSST)を求め、実測値との比較により 10 日間でのコンポジット画像の適用可能性を検証した。1997 年 10 月 7 日及び 10 月 16 日の sea surface temperature の予測値と実測値との差は長江河口域においてほとんどの地点で 0.5℃以内(最大の相異も 1℃以内) であった。このことから得られたコンポジット画像は、東シナ海全域の海域環境を再現しており雲の影響を除去するのに有効であることが判明した。

また、ランドサット衛星画像 TM データを用いた長江河口域における生態系観測を試みた。観測項目として Chl.a、浮遊粒子、表面水温(SST)を選択し、1997 年 10 月 13 日の TM データによってそれらの推定を行った。TM 可視バンドを用いて Chl.a と浮遊粒子の推定を、そして TM バンド６を用いて SST を推定した。大気による吸収、散乱と太陽光による閃光の影響を受けている TM 可視光の大気補正に 6S コードを適用した。より広域のデータを用いた相関関係を求めるために、1997 年 10 月 9 日の SeaWIFS データから得た Chl.a 値を用いた。この結果、相関式として log (Chl-a) = 0.752－ 4.79log (TM1/TM2)を得た。同様に浮遊粒子については log(S)=2.7 + 1.06 log R(660、TM4) が得られた。SST についてはTM バンド６を用いて求めた値と Split-Window 法により NOAA データから得られた値を 1997 年 10 月 13 日について求め比較した。この結果両者の差は 0.386℃と小さく良好な結果が得られた。

[キーワード]　AVHRR, East China Sea, SST, TM, Chlorophyll-a, Suspended Solids, 6S

D-1.3.3 Estimation of Environmental Load Through Large River in East China Sea

Contact Person Masataka Watanabe
Director,
Division of Water and Soil Environment
National Institute for Environmental Studies
Environment Agency
16-2 Onogawa, Tsukuba, Ibaraki 305, Japan
Tel.: 81-298-50-2338, Fax: 81-298-50-2576
E-mail: masawata@nies.go.jp

Total Budget for FY1997-FY1998 **3,525,000 Yen (FY1998; 1,765,000 Yen)**

Abstract

The research focuses on using TM data to monitor water quality in the Changjiang estuarine region. Two representative water quality parameters, chlorophyll-a and suspended solids, are estimated from the TM 117-38,39 on Oct.13, 1997. 6S code is applied to do atmosphere correction for TM visible bands which is taking gaseous absorption, atmosphere scattering and sun glint into account. The relation analysis suggests the band ratio of log(TM1/TM2) has the largest coefficient with the log(Chlorophyll-a) provided by SeaWiFs on Oct. 9, 1997. Based on this, the linear regression equation: log(chlorophyll-a) = 0.752 – 4.79 * log (TM1/TM2) (R = -0.697) is applied to the whole two scenes. Similarly, the commonly used equation log (S) = 2.7 + 1.06 log R(660, TM4) is applied to estimate the suspended solids.

Keywords: TM, Chlorophyll-a, Suspended Solids, 6S

1. Introduction

Water quality refers to chemical, physical and biological characteristics of water. The chemical characteristics include the organic and inorganic substances like heavy metals, pesticides, detergents and petroleum. The physical characteristics consists of turbidity, colour and temperature, the biological mainly include plankton and pigment (Lo, 1986). The traditional way to get the knowledge of these water quality parameters, chlorophyll a, suspended solids, salinity, temperature and so, is using point-sampling methods. Though it may provide precise measurement for a point, it is far from satisfactory when a synoptic and large coverage is preferred, especially for those parameters with rapid fluctuations and considerable spatial variations.

Remote sensing data provides another choice. Since the early 1970s a large number of researchers have used satellite and airborne sensors to estimate and map water quality parameters because of their abilities in providing synoptic views and better estimates of spatial distribution (Ekstrand, 1992). The data of Landsat Multispectral Scanner (MSS), Nimbus Coastal Zone Colour Scanner (CZCS), NOAA Advanced Very High Resolution Radiometer (AVHRR), and newly developed Sea-viewing Wide Field-of-view Sensor (SeaWiFs) are widely used to deduce the water quality parameters (Alfoldi and Munday, 1978; Khorram and Cheshire, 1985; Lindell et al., 1986; Ritchie et al., 1987; Hooker et al., 1992).

The Thematic Mapper TM scanner is a sensor mountained on the Landsat 5 satellite with the higher spatial, spectral and radiometric resolution than MSS. There are seven bands in it: Band 1 450-520nm, Band 2 520-600nm, Band 3 630-690nm, Band 4 760-900nm, Band 5 1.55-1.74μm, Band 6 10.4-12.5μm, and Band 7 2.08-2.35μm. The spatial resolution of TM is 28.5 × 28.5m for all bands except the Band 6, which has a spatial resolution of 120m.

Though Landsat TM was originally designed for land observations, it does elicit information concerning the water quality and thus can be used to deduce those parameters(Dekker and Peters, 1992).

There are a sum of references concerning the application of TM data in water quality monitoring. For chlorophyll-a, Kim and Linebaugh (1985) found that TM data could be used to quantify it in the range of 0.5 to 2.0 mg/m3. Dwivedi and Narain (1987) obtained a coefficient of determination of 0.68 with a phytoplankton pigment range (chlorophyll-a + phaeophytin-a) of 0.5 to 4.1 mg/m3 in ocean waters. Tassan (1987) proposed that TM data could provide quantitative information of acceptable quality on chlorophyll-a in sea water within 0.1 to 17 mg/m3 and also pointed out that this estimation may be unreliable close to the coast where the sediment content is high. Ekstrand (1992) suggested that a ratio of TM bands TM1/(logTM3 + 1) should be used in waters influenced by terrigenous influx to quantify chlorophyll-a. Suspended solids, turbidity, salinity are also got with various degree of success using regression analysis in different regions (Baban, 1997; Braga et al, 1993; Dekker and Peters, 1993; Foster et al, 1993).

The paper selects two water quality parameters (chlorophyll-a and suspended solids) and tries to deduce them from TM data. They are estimated following the way proposed by Tassan (1987) but using different atmosphere correction way.

2. Research region and TM data

Changjiang River catchment covers 1.8 million km^2 and there are nearly 300 million people. With the rapid industrialization and growth of population, the disturbance to water cycle become more and more serious. Together with outputting polluted materials, it is sure that will impact on the marine ecosystems in the East China Sea. Recent researches have shown that coastal ocean responses to such loadings are likely to occur within the 100-year time frame which indicates the important of this research.

The Changjiang estuarine area is one jointly acted by the diluted water, Taiwan Warm current, cold water mass of the Yellow Sea and the offshore current of the East China Sea. Large amounts of nutrients carried by the various currents, particularly by the Changjiang River make the area one of the most productive.

Two continuous scenes of TM data on Oct. 13, 1997 which cover this area are selected as the source to estimate water quality. They are path 117, row 38 and 39. The passing time is around 01:52 (GT). The location of the scenes is shown in Fig. 1.

3. Atmosphere correction

The radiance recorded by the TM sensor is the combination of water-leaving radiance and those scattered by the air (Rayleigh Scattering) and by microscopic particles suspended in the air (Mie Scattering). Gordon et al (1983) proposed that the sensor radiance $L_0(\lambda)$ can be simply divided into its components by ignoring the direct sun glint and assuming that the sea surface is flat when dealing with CZCS data:

$$L_t(\lambda) = L_r(\lambda) + L_a(\lambda) + t(\lambda)L_w(\lambda) \qquad (1)$$

L_r and L_a are given by

$$L_x = \omega_x(\lambda)\gamma_x(\lambda)F_0'(\lambda)p_x(\theta,\theta_0,\lambda)/4\pi, \qquad (2)$$

where

$$P_x(\theta,\theta_0,\lambda) = \{P_x(\theta_-,\lambda) + [\rho(\theta) + \rho(\theta_0)]P_x(\theta_+,\lambda)\}/\cos\theta \qquad (3)$$

$$\cos\theta_\pm = \pm\cos\theta_0\cos\theta + \sin\theta_0\sin\theta\cos(\phi - \phi_0) \qquad (4)$$

θ_0 and ϕ_0 are the solar zenith and azimuth angles respectively, θ and ϕ are the zenith and azimuth angles of the sensor. $\rho(\theta)$ is the Fresnel reflectance of the interface for an incident angle θ, $P_x(\theta,\lambda)$ is the scattering phase function of component x (x = r or a) at λ, $\omega_x(\lambda)$ is the single-scattering albedo of x (ω_r = 1), and $\tau_x(\lambda)$ is the optical thickness of x. $F'_0(\lambda)$is the instantaneous extraterrestrial solar irradiance $F_0(\lambda)$ reduced by two trips through the ozone layers, and can be calculated as the following function:

$$F_0' = F_0\exp\left[-\tau_{Oz}\left(\frac{1}{\cos\theta} + \frac{1}{\cos\theta_0}\right)\right] \qquad (5)$$

Eq.(1) was further developed as:

$$L_w(\lambda) = \frac{1}{T_{(\lambda)}}\{L(\lambda) - L_R(\lambda) - \varepsilon(\lambda,\lambda_0)[L(\lambda_0) - L_R(\lambda_0) - L_w(\lambda_0)T(\lambda_0)]\} \qquad (6)$$

where $L_w(\lambda)$is the water upwelling radiance; T is the diffuse transmittance of the atmosphere; L_R represents Rayleigh path-radiance; λ is the central wavelength of the sensor band; $\varepsilon(\lambda,\lambda_0) = L_A(\lambda) / L_A(\lambda_0)$, where L_A is the aerosol path-radiance; λ_0 = 670nm (CZCS band 4). $\varepsilon(\lambda, 670)$ can be evaluated from remotely-measured data pertaining to 'clear water' areas (i.e. with chlorophyll-a lower than $0.2mg/m^3$).

Eq. (6) has been further applied to TM data to do atmosphere correction by Tassan (1987). Moreover, TM band 4 (λ = 838 nm) is used as λ_0 besides the TM band 3, which is substantially equivalent to radiance measured by CZCS band 4 (λ = 670nm, $\Delta\lambda$ = 20 nm).

Ignoring the direct sun glint will not cause big error for the CZCS data since CZCS tilts away from the Sun thus avoid the direct sun glint in all circumstances. But TM do not have such design and faces to the nadir, therefore will be affected by the sun glint. Tassan (1987) also noticed such problem when expanded eq. (4) into TM data. His error analysis suggests that this effect can not be neglected for TM data, especially the wind distribution is not uniform over the TM scene. For example, under maximum sun elevation, an assumed wind speed of 6m/s in the clear-water zone selected for the determination of the $\varepsilon(\lambda,\lambda_0)$ while other area has the speed of 5m/s, the error can be in the ranges from +20 percent to –50 percent for 2 < chlorophyll-a < 10 mg/m^3 and +60 percent to +10 percent for 0.4 < S < 10 g/m^3. But the error will be somehow lower when the wind speed is constant (Tassan, 1987). Another problem arises when TM band 4 is used as λ_0 since in this band width includes the 800 nm water vapor absorption level (Kondratyev, 1969), which will cause the reduction in the measured radiance. The paper applies 6S code to do atmosphere correction for TM data. 6S code was developed by Vermote et al (1997) to be used to predict the satellite signal from 0.25 to 4.0 micrometers. Besides the above mentioned scattering effects (Rayleigh and aerosol scattering), 6S code also takes gaseous absorption and sun glint into account.

For gaseous absorption in the solar spectrum is principally due to oxygen, ozone, water vapor, carbon dioxide, methane and nitrous oxide. O_2, CO_2, CH_4, and N_2O are assumed constant and uniformly mixed in the atmosphere, while the variable H_2O and O_3 concentrations are treated more carefully in 6S code. The random exponential band model of Goody (1964) is selected to simulate for H_2O and that of Malkmus (1967) for other gases.

In 6S, the sun glint is computed exactly with the Snell-Fresnel laws. For a rough sea surface, the reflection is conditioned by the wind and be computed numerically by many facets whose slopes are described by a Gaussian distribution. The basic flow of 6S code is shown as Fig. 2 (Vermote et al, 1997). In case of TM 117-38,39 scenes, the following results are obtained. (Table 1).

Table 1 Outputs of 6S code on the case of TM 117-38,39 scenes (Oct. 13, 1997),

(the atmospherically corrected reflectance of each band is calculated as R = y / (1 + cy), where y = a * measured radiance – b; a, b)

TM Bands	A	B	C
1	0.00291	0.09665	0.15552
2	0.00306	0.05444	0.10531
3	0.00337	0.03162	0.07678
4	0.00495	0.01699	0.05320
5	0.02408	0.00664	0.03245
7	0.06560	0.00500	0.02743

4. Chlorophyll-a

Chlorophyll-a is the pigment presenting in living plants responsible for photosynthesis. In the ocean, it lies in phytoplankton and is usually taken as a measure of phytoplankton biomass.

Many algorithms have been proposed to extract chlorophyll-a from water-leaving radiance $L_w(\lambda)$ based on the ratio of the water-leaving radiance at two different wavelengths (Gordon et al., 1983). The basis for this lies in the fact that in the first approximation L_w is proportional to the ratio of the backscattering coefficient b_b and the absorption coefficient a of the water plus its constituents, i.e., $L_w \sim b_b/a$. Both a and b_b are linearly summable over the constituents, and the portion of a and b_b arising from photoplankton pigments is proportional to chlorophyll-a concerntration. These pigments strongly influence a but have little effect on backscattering, which primarily results from interactions with photoplankton detrital material and inorganic suspended material of nonbiogenic origin. Thus the ratio of the water-leaving radiance at two wavelengths will be approximately inversely proportional to the ratio of the associated absorption coefficients.

According to this, a basic algorithm can be got:

$$\log C = A + B \log R(i, j) \tag{7}$$

where C refers to Chlorophyll-a concentration; R(i, j) is the ratio of the water-leaving radiance of band i and band j; A and B are the coefficients which can be decided by linear regression analysis. Though eq.(7) is firstly developed for CZCS data, Tassan (1987) expanded it to TM data. This paper follows the same philosophy and applies eq.(7) to the TM data. The ratio of TM1/TM2, TM4/TM3, TM1/(logTM3 + 1) and TM band 1 to 4 are used in relation analysis in order to find out the best fit curve in this region. Since no corresponding site measuring data are available, SeaWiFs chlorophyll-a data on Oct. 9, 1997 are used as original data.

SeaWiFs, the Sea-viewing Wide Field-of-view Sensor, is a new and successor of CZCS to monitor the ocean color (Hooker et al., 1992). The quality of estimated chlorophyll-a is within ± 35% (McClain et al., 1995), and with 4 Km spatial resolution.

Thirty seven chlorophyll-a data are randomly picked out from the SeaWiFs data and be used in relation analysis with corrected TM band 1 to 4 and above listed ratios of the corresponding sites in the TM scenes. The result is listed in Table 2.

Table 2 The coefficients between log (chlorophyll-a) and TM Band 1 to 4 and band ratios

Factors	R	P
TM 1	0.60562	< 0.0001
TM 2	0.64035	< 0.0001
TM 3	0.51544	0.0011
TM 4	0.44416	0.00589
TM 1 / TM 2	-0.697	< 0.0001
TM 4 / TM 3	-0.51747	0.00104
TM 1 / (log TM 3 + 1)	0.01794	0.91609

From Table 2, we can see the band ratio of TM1/TM2 is the best choice to estimate chlorophyll-a. Fig. 3 shows the regression analysis result, thus eq.(7) can be determined as:

$$\log(\text{chlorophyll-a}) = 0.752 - 4.79 * \log(\text{TM1/TM2}) \quad (R = -0.697) \qquad (8)$$

Figure 3 The relation between the log(chlorophyll-a) and log(TM1/TM2).

(The regression analysis was based on 37 randomly collected samples from the TM 117-38,39 scenes on Oct. 13, 1997.)

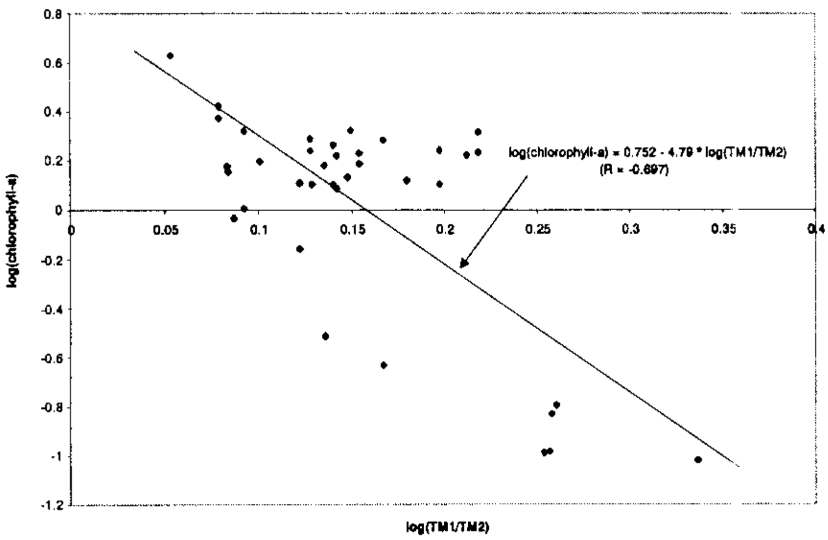

The relation coefficient R is not so high as reported by others. Two factors may contribute to this. One is the time difference between SeaWiFs data and TM data, and the another is the difference of spatial resolution between them. This need further study.

The regression eq. (6) is applied to the scenes and the distribution of chlorophyll-a on Oct. 13, 1997 in the estuarine region is shown as Fig. 4.

5. Suspended solids

Several papers have reported how to estimate suspended solids using TM data (e.g. Khorram and Cheshire, 1985; Tassan, 1987). And the results have been favorable and therefore no attempts were made to develop a new algorithm for estimating suspended solids (Ekstrand, 1992). Thus suspended solids here is estimated with TM data using the algorithm developed by Tassan (1987):

$$\log(S) = 2.7 + 1.06 \log R\,(660, \text{TM4}) \qquad (9)$$

Thus the spatial distribution of suspended solids can be got by applying the eq. (9) to the scenes (Fig. 5).

6. Conclusion

Though Landsat TM was originally designed for land observations, it does elicit information concerning the water quality and thus can be used to deduce those parameters, for instance, chlorophyll-a, suspended solids and sea surface temperature. 6S code takes gaseous absorption, Rayleigh and aerosol scattering, and sun glint into account which is suitable to be applied to do atmosphere correction for TM data. The relation analysis shows the band ratio of TM1/TM2 can provide the best curve for estimating chlorophyll-a in the Changjiang estuarine area, while TM 2 for suspended solids.

References

Alfoldi, T. T., and Munday, J. C., 1978. Water quality analysis by digital chromaticity mapping of Landsat data. Canadian Journal of Remote Sensing, 4, 108-126.

Baban, S. M. J., 1997. Environmental monitoring of estuaries; estimating and mapping various environmental indicators in Breydon Water Estuary, U. K., using Landsat TM imagery. Estuarine, coastal and shelf science, 44, 589-598.

Braga, C. Z. F., Setzer, A. W., and Lacerda, L. D. 1993. Water quality assessment with simultaneous landsat-5 TM data at Guanabara Bay, Rio de Janeiro, Brazil. Remote Sensing of Environment, 45, 95-106.

Dekker, A. G., and Peters, S. W., 1993. The use of Thematic Mapper for the analysis of eutrophic lakes: a case study in the Netherlands. International Journal of Remote Sensing, 14, 799-821.

Dwivedi, R. M., and Narain, A., 1987. Remote sensing of phytoplankton, An attempt from the Landsat Thematic Mapper. International Journal of Remote Sensing, 8, 1563-1569.

Ekstrand, S., 1992. Landsat TM based quantification of chlorophyll-a during algae blooms in coastal waters. International Journal of Remote Sensing, 13, 1913-1926.

Forster, B. C., Sha X. and Xu B., 1993. Remote sensing of sea water quality parameters using Landsat-TM. International Journal of Remote Sensing, 14, 2759-2771.

Goody, R. M., 1964. Atmospheric radiation 1, theoretical basis. Oxford University Press, 436pp.

Gordon, H. R., Clark, D. K., Brown, J. W. et al., 1983. Phytoplankton pigment concentrations in the Middle Atlantic Bight: comparison of ship determinations and CZCS estimates. Applied Optics, 22, 20-36.

Hooker, S. B., Esaias, W. E., Feldman, G. C. et al., 1992. NASA Technical Memorandum 104566, Vol. 1, An Overivew of SeaWiFs and Ocean Color.

Khorram, S., and Cheshire, M. S., 1985. Remote sensing of water quality in the Neuse river estuary, North Carolina. Photogrammetric Engineering and Remote Sensing, 51, 329-341.

Kim, H. H., and Linegaugh, G., 1985. Early evaluation of Thematic Mapper data for coastal process studies. Advances in Space Research, 5, 21-29.

Lindell, T., Karlsson, B., Rosengren, M., and Alfoldi, T., 1986. A further development of the chromaticity technique for satellite mapping of suspended sediment load. Photogrammetric Engineering and Remote Sensing, 52, 1521-1529.

Lo, C. P., 1986. Applied Remote Sensing. Longman Scientific and Technical, London.
Malkmus, W., 1967. Ramdon Lorentz band model with exponential- tailed S-1 line-intensity distribution function. J. Opt. Soc. Am., 57, 323-329.
McClain, C. R., Arrigo K., Esaias, W. E. et al., 1995. NASA Technical Memorandum 104566, Vol. 28, SeaWiFs Algorithms, Part 1.
Ritchie, J. C., Cooper, C. M., and Yongqing, J., 1987. Using Landsat Multispectral Scanner data to estimate suspended sediments in Moon Lake, Mississippi. Remote sensing of Environment, 23, 65-81.
Tassan, S., 1987. Evaluation of the potential of the Thematic Mapper for marine application. International Journal of Remote Sensing, 8, 1455-1478.
Vermote, E., Tanre, D., Deuze, J. L. et al., 1997. 6S user guide version 2.

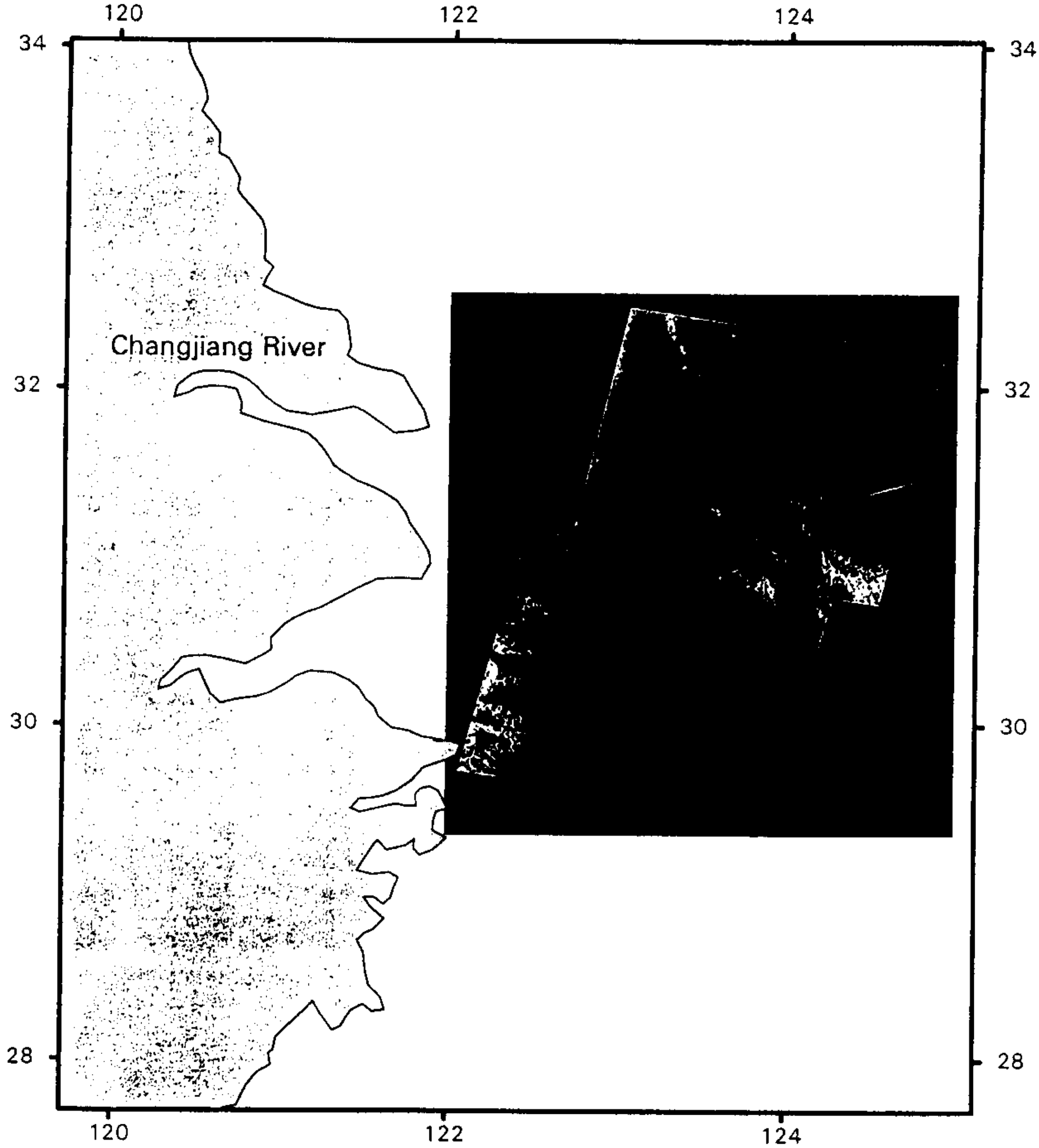

Figure 1 Location of TM 117-38,39 Scenes

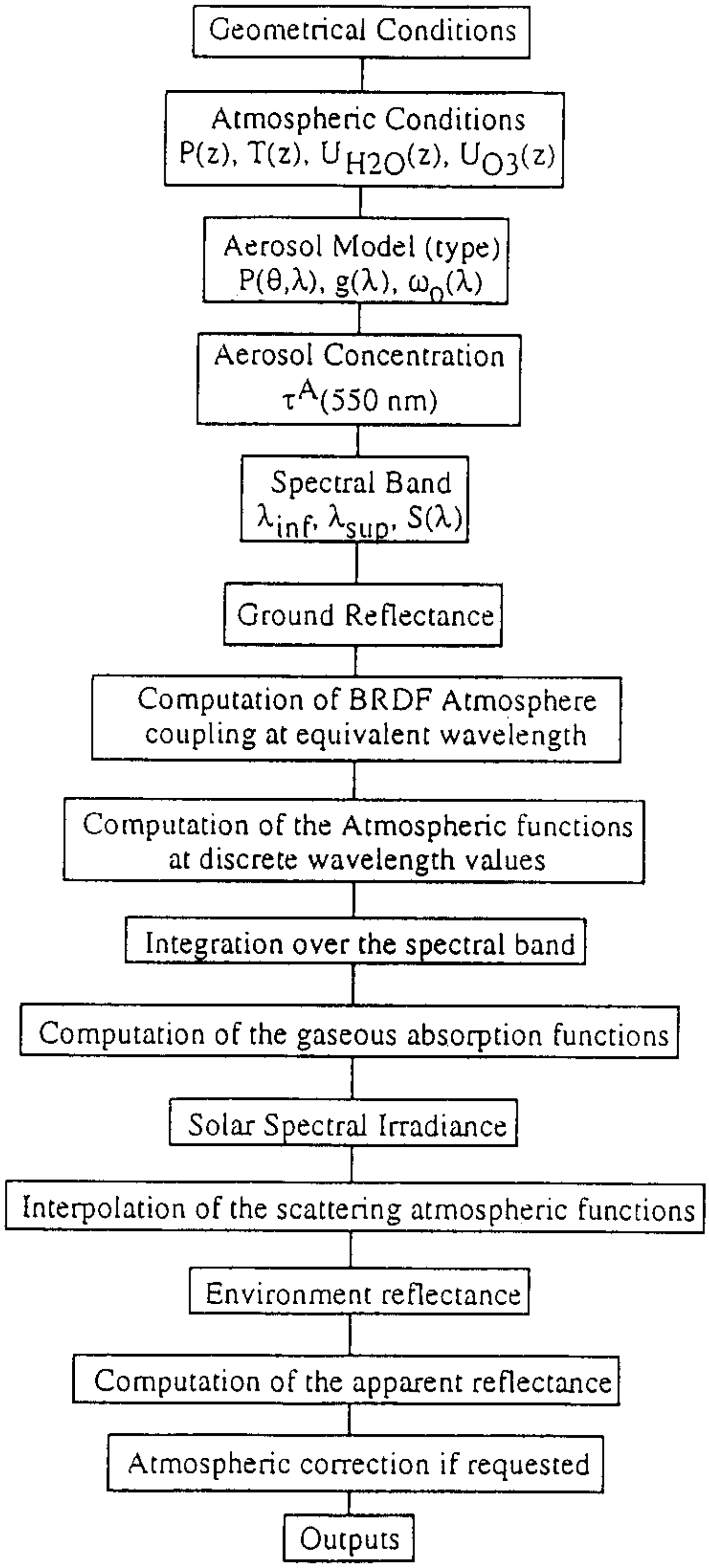

Figure 2 General flow chart 6S computations

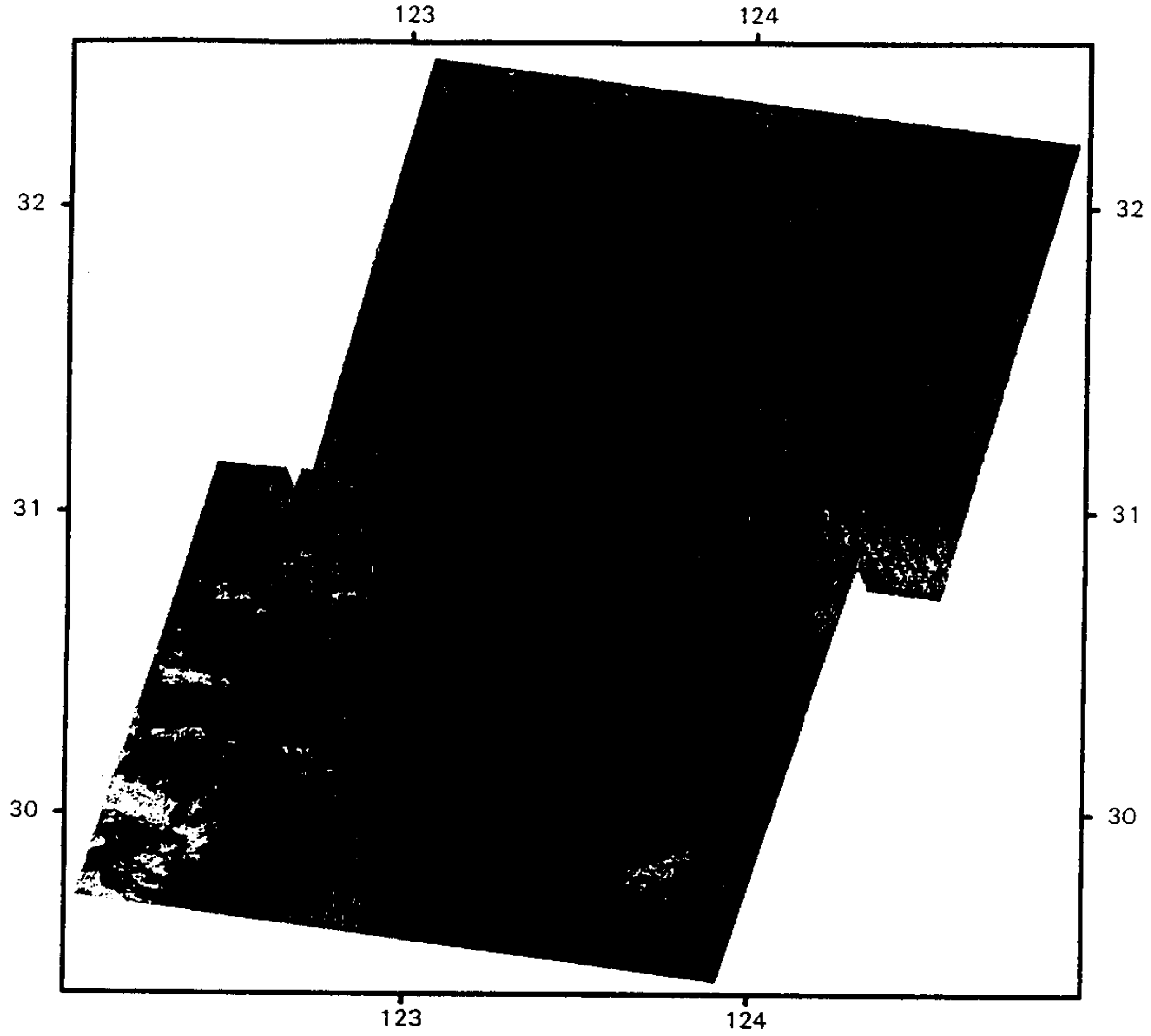

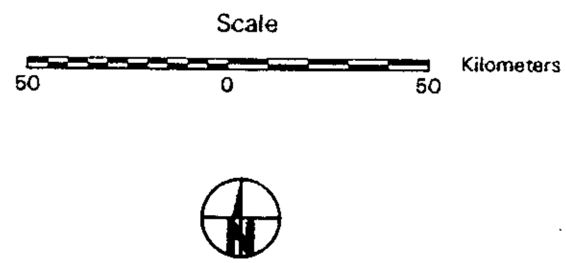

Figure 4

Distribution of Chlorophyll a on Oct. 13, 1997

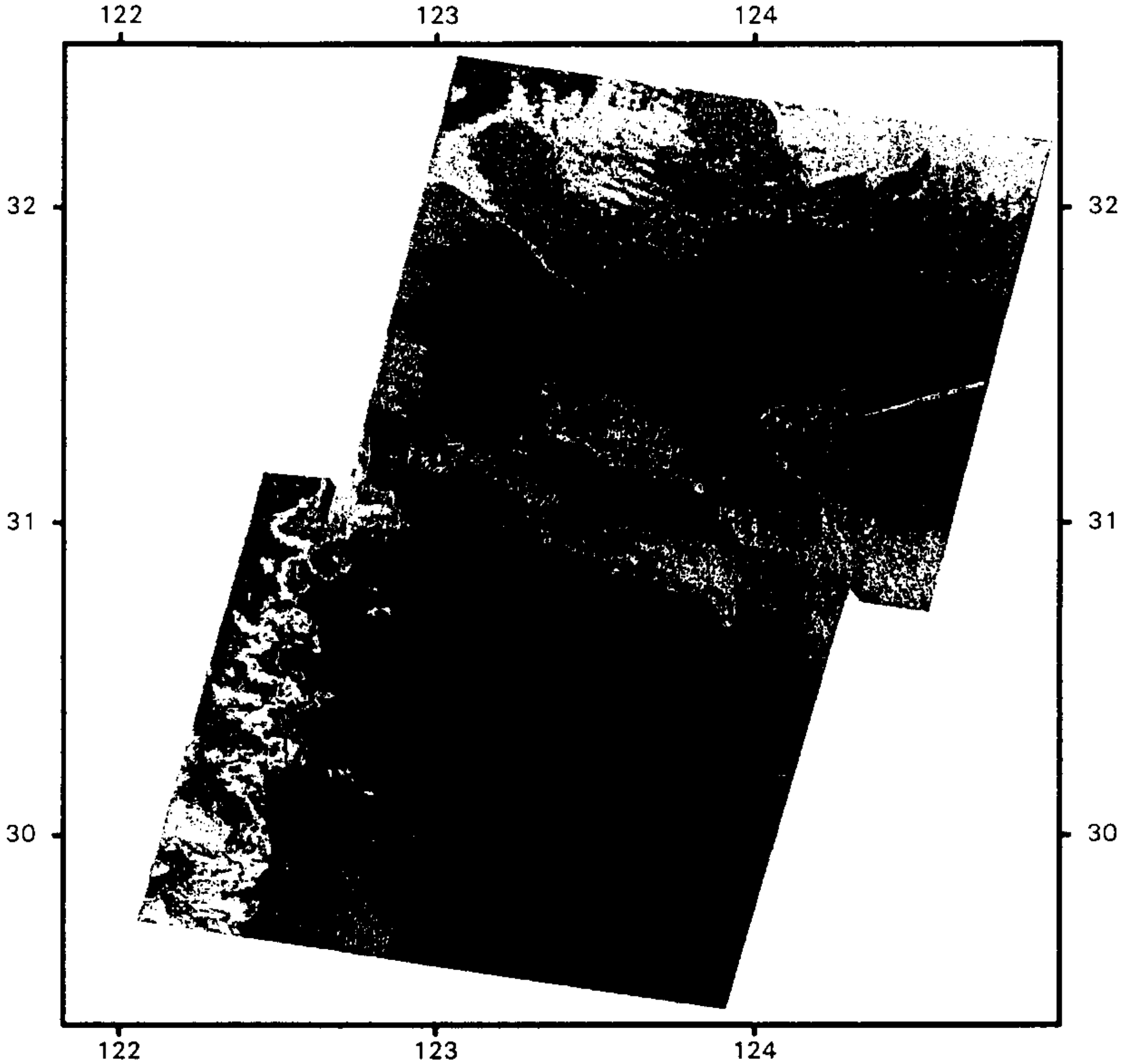

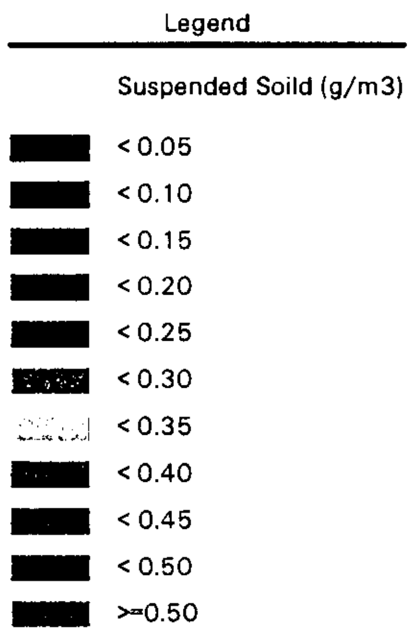

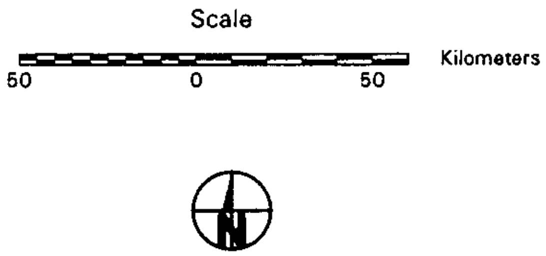

Figure 5

Distribution of Suspended Solids
on Oct. 13. 1997